4254 *Inorg. Chem.* **1984**, *23*, 4254–4261

Contribution from the Laboratorium für Anorganische Chemie, ETH-Zentrum, CH-8092 Zürich, Switzerland, and Istituto di Chimica Farmaceutica, Università di Milano, I-20131 Milano, Italy

New Cationic Rhodium(I)–Iridium(III) Complexes with Bridging Hydride and Chloride Ligands. Synthesis and X-ray Crystal Structure of $[(\text{diphos})\text{Rh}(\mu\text{-H})(\mu\text{-Cl})\text{IrCl}(\text{PEt}_3)_3]\text{BF}_4$ and $[(\text{diphos})\text{Rh}(\mu\text{-H})(\mu\text{-Cl})\text{IrH}(\text{PEt}_3)_3]\text{BF}_4$

HANS LEHNER,[1a,b] DOMINIQUE MATT,[1a] ANTONIO TOGNI,[1a] RENE THOUVENOT,[1a] LUIGI M. VENANZI,*[1a] and ALBERTO ALBINATI[1c]

Received December 15, 1983

Reaction of $[(\text{diphos})\text{Rh}(\text{acetone})_2]\text{BF}_4$ with *mer,trans*-IrHCl_2L_3 (L = PMe_2Ph, PEt_2Ph, PEt_3; diphos = $\text{Ph}_2\text{PCH}_2\text{CH}_2\text{PPh}_2$) affords the hydrido-bridged dinuclear complexes $[(\text{diphos})\text{Rh}(\mu\text{-H})(\mu\text{-Cl})\text{IrClL}_3]\text{BF}_4$. Solution studies show that the bridging ligands are only weakly coordinated to the rhodium. The molecular structure of **3** (L = PEt_3) has been determined by X-ray diffraction: monoclinic, space group $P2_1/c$, $Z = 4$, $a = 11.786$ (2) Å, $b = 19.673$ (4) Å, $c = 22.571$ (4) Å, $\beta = 89.88$ (1)°. The structure was solved by Patterson and Fourier methods using 5750 observed reflections [$I \geq 3\sigma(I)$] and refined to a conventional $R = 0.057$. The coordination around rhodium is distorted square planar and that around iridium is distorted octahedral. The Rh–Ir distance is 2.903 (1) Å, and the bridging chlorine atom is almost symmetrically bonded to the metals (Rh–Cl = 2.386 (3), Ir–Cl = 2.381 (3) Å). The isoelectronic complex $[(\text{diphos})\text{Rh}(\mu\text{-H})(\mu\text{-Cl})\text{IrH}(\text{PEt}_3)_3]\text{BF}_4$ was obtained in a similar reaction, starting from *mer,cis*-$\text{IrH}_2\text{Cl}(\text{PEt}_3)_3$. Its structure determined by X-ray diffraction, as above, is monoclinic, space group $P2_1$, $Z = 2$, $a = 11.102$ (2) Å, $b = 13.582$ (3) Å, $c = 16.694$ (4) Å, $\beta = 85.06$ (2)°. The final agreement factor (for the 4553 observed reflections) R is 0.062. As for compound **3** the coordination around Rh and Ir is distorted square planar and octahedral, respectively. There is a pronounced asymmetry in the chlorine bridge (Rh–Cl = 2.394 (5), Ir–Cl = 2.510 (5) Å), and the metal–metal separation is 2.969 (2) Å.

Introduction

Hydrido-bridged complexes have shown to be precursors of hydrogenation catalysts.[2-4] The current interest in heterobimetallic systems of this type results from the search of new or more selective hydrogen-transfer reactions.[5] From our previous synthetic studies it appears that the schematic formulation of hydrido-bridged complexes shown in eq 1 may be

$$\underset{\text{acceptor}}{\text{L}_m\text{M}(\text{solvent})} + \underset{\text{donor}}{\text{L}_n\text{M}'\text{H}} \rightarrow \text{L}_p\text{M}(\mu\text{-H})\text{M}'\text{L}_q \qquad (1)$$

used successfully for the preparation of a great variety of new bimetallic hydrido complexes.[6,7] In this paper we describe some new uses of this Lewis acid–Lewis base concept applied to the synthesis of cationic Rh(I)–Ir(III) complexes.

Experimental Section

All operations were carried out under purified nitrogen. Solvents were distilled under nitrogen and dried prior to use. Elemental analyses were formed by the Microanalytical Section of the Swiss Federal Institute of Technology. Infrared spectra in the region 4000–400 cm^{-1} were recorded on a Beckman IR 4250 spectrophotometer as KBr pellets or Nujol mulls. The ^{1}H and $^{31}\text{P}\{^1\text{H}\}$ NMR spectra were recorded at 90.00 and/or 250.00 and 36.43 MHz, respectively, on a FT Bruker WH-90 or FT Bruker 250 instrument. ^{1}H and ^{31}P chemical shifts are given relative to external $(\text{CH}_3)_4\text{Si}$ and H_3PO_4, respectively. A positive sign denotes a shift downfield of the reference.

A. Syntheses. $[\text{Rh}(\text{diphos})(\text{nbd})]\text{BF}_4$[8] (nbd = norbornadiene), *mer,trans*-IrHCl_2L_3 (L = PMe_2Ph, PEt_2Ph, PEt_3),[9] and *mer,cis*-$\text{IrHCl}_2(\text{PMePh}_2)_3$,[10] were prepared according to literature methods. For the preparation of *mer,cis*-$\text{IrH}_2\text{Cl}(\text{PEt}_3)_3$, a toluene solution of $[(\text{coc})_2\text{IrCl}]_2$ (coc = cyclooctadiene) was reacted with 3 equiv of PEt_3, and hydrogen was bubbled through the solution for 10 min, leading almost quantitatively to the product.

$[(\text{diphos})\text{Rh}(\mu\text{-H})(\mu\text{-Cl})\text{IrCl}(\text{PMe}_2\text{Ph})_3]\text{BF}_4$ (1). To a solution of *mer,trans*-$\text{IrHCl}_2(\text{PMe}_2\text{Ph})_3$ (0.122 g, 0.18 mmol) in acetone (20 mL) was added at −78 °C a solution of $[(\text{diphos})\text{Rh}(\text{acet})_2]\text{BF}_4$[11] (acet = acetone) (prepared by hydrogenation of a solution of $[(\text{diphos})\text{Rh}(\text{nbd})]\text{BF}_4$ (0.123 g, 0.18 mmol) in 15 mL of acetone). The reaction mixture immediately became red, and the solution was stirred for 2 h at room temperature. After addition of pentane, the product precipitated as a brick red powder. It was then recrystallized from a concentrated methanol solution at −20 °C: yield 0.185 g (81%); mp 158 °C dec. Anal. Calcd for $\text{C}_{50}\text{H}_{58}\text{BCl}_2\text{F}_4\text{IrP}_5\text{Rh}$: C, 47.41; H, 4.62. Found: C, 47.45; H, 4.64. ^{1}H NMR (CD_2Cl_2): δ −13.3 (d of complex m, 1 H, μ-H, $^2J(\text{HP}_c) = 93$ Hz), 1.32 (d, 6 H, $(H_3\text{C})_2\text{P}_c$, $^2J(\text{PH}) = 10.9$ Hz), 1.45 and 1.49 (two virtual t, 12 H, $\text{C}H_3\text{P}_{d,e}$, $^{4+2}J(\text{PH}) = 7$ Hz), 2.5 (center of a complex m, 4 H, diphos), 6.9–8.0 (aromatic H). $^{31}\text{P}\{^1\text{H}\}$ NMR (CD_2Cl_2): δ −48.7 (d, $\text{P}_{d,e}$, $^2J(\text{P}_{d,e}\text{P}_c) = 19$ Hz), −38.7 (complex m, P_c, $^2J(\text{P}_c\text{P}_d) = 19$ Hz, $^4J(\text{P}_c\text{P}_a) = 49$ Hz), 68.4 (ddd, P_a, $^1J(\text{P}_a\text{Rh}) = 182$ Hz, $^2J(\text{P}_a\text{P}_b) = 38$ Hz, $^4J(\text{P}_a\text{P}_c) = 49$ Hz), 80.5 (ddd, P_b, $^1J(\text{P}_b\text{Rh}) = 197$ Hz, $^2J(\text{P}_bP_a) = 38$ Hz, $^4J(\text{P}_b\text{P}_c) = 3$ Hz).

$[(\text{diphos})\text{Rh}(\mu\text{-H})(\mu\text{-Cl})\text{IrCl}(\text{PEt}_2\text{Ph})_3]\text{BF}_4$ (2). To a solution of *mer,trans*-$\text{IrHCl}_2(\text{PEt}_2\text{Ph})_3$ (0.115 g, 0.15 mmol) in acetone (25 mL) was added at −78 °C a solution of $[(\text{diphos})\text{Rh}(\text{acet})_2]\text{BF}_4$ (prepared from 0.102 g of $[(\text{diphos})\text{Rh}(\text{nbd})]\text{BF}_4$). The solution immediately turned red and was then stirred for 2 h at room temperature. After addition of cold pentane, the product precipitated as a brick red powder. It was recrystallized from methanol at −20 °C, affording red crystals: yield 0.146 g (73%); mp 155 °C dec. Anal. calcd for $\text{C}_{56}\text{H}_{60}\text{BCl}_2\text{F}_4\text{IrP}_5\text{Rh}$: C, 50.17; H, 4.51. Found: C, 50.09; H, 4.61. ^{1}H NMR (CD_2Cl_2): δ −14.2 (d of complex m, 1 H, μ-H, $^2J(\text{HP}_c) = 90$ Hz), 0.4 (m, 12 H, $\text{C}H_3\text{CH}_2$), 0.9 (m, 8 H, $\text{C}H_2\text{CH}_3$), 1.9 (m, 6 H, $\text{C}H_3\text{CH}_2\text{P}_c$), 2.2 (m, 4 H, $\text{C}H_2\text{P}_c$), 2.5 (m, 4 H, diphos), 6.9–8.1 (aromatic H). $^{31}\text{P}\{^1\text{H}\}$ NMR (CD_2Cl_2): δ −31.2 (d, $\text{P}_{d,e}$, $^2J(\text{P}_{d,e}\text{P}_c) = 15$ Hz), −24.8 (complex m, P_c, $^2J(\text{P}_c\text{P}_d) = 15$ Hz, $^4J(\text{P}_c\text{P}_a) = 46$ Hz), 67.0 (two pseudotriplets (ddd), P_a, $^1J(\text{P}_a\text{Rh}) = 181$ Hz, $^2J(\text{P}_a\text{P}_b) = 42$ Hz, $^4J(\text{P}_a\text{P}_c) = 46$ Hz), 78.6 (ddd, P_b, $^1J(\text{P}_b\text{Rh}) = 198$ Hz, $^2J(\text{P}_b\text{P}_a) = 42$ Hz, $^4J(\text{P}_b\text{P}_c) = 2$ Hz).

$[(\text{diphos})\text{Rh}(\mu\text{-H})(\mu\text{-Cl})\text{IrCl}(\text{PEt}_3)_3]\text{BF}_4$ (3). A solution of $[(\text{diphos})\text{Rh}(\text{acet})_2]\text{BF}_4$ in 15 mL of acetone (prepared from 0.245 g (0.36 mmol) of $[(\text{diphos})\text{Rh}(\text{nbd})]\text{BF}_4$) was added at −78 °C to a solution of *mer,trans*-$\text{IrHCl}_2(\text{PEt}_3)_3$ (0.223 g, 0.36 mmol) in acetone (20 mL). The reaction mixture turned red and was stirred for 2 h at room temperature. After concentration of the solution and addition of cold pentane under vigorous stirring, the product precipitated as a brick red powder. Recrystallization from methanol gave red crystals: yield 0.347 g (80%); mp 145 °C. Anal. Calcd for $\text{C}_{44}\text{H}_{70}\text{BCl}_2\text{F}_4\text{IrP}_5\text{Rh}$:

---

(1) (a) ETH-Zentrum. (b) Taken in part from the Ph.D. thesis of H.L. (c) University of Milano.

(2) Gill, D. S.; White, C.; Maitlis, P. M. *J. Chem. Soc., Dalton Trans.* **1978**, 617.

(3) Maitlis, P. M. *Acc. Chem. Res.* **1978**, 301.

(4) Lehner, H.; Musco, A.; Venanzi, L. M.; Albinati, A. *J. Organomet. Chem.* **1981**, *213*, C46.

(5) Collman, J. P.; Hegedus, L. S. "Principles of Organotransition Metal Chemistry"; University Science Books: Mill Valley, CA, 1980.

(6) Venanzi, L. M. *Coord. Chem. Rev.* **1982**, *43*, 251.

(7) Lehner, H.; Matt, D.; Pregosin, P. S.; Venanzi, L. M.; Albinati, A. *J. Am. Chem. Soc.* **1982**, *104*, 6825.

(8) Schrock, R. R.; Osborn, J. A. *J. Am. Chem. Soc.* **1971**, *93*, 3089.

(9) Chatt, J.; Coffey, R. S.; Shaw, B. L. *J. Chem. Soc. A* **1965**, 7391.

(10) Angoletta, M. *Gazz. Chim. Ital.* **1969**, *99*, 46.

(11) Halpern, J.; Riley, B. P.; Chan, A. S.; Pluth, J. J. *J. Am. Chem. Soc.* **1977**, *99*, 8055.

C, 43.79; H, 5.85. Found: C, 44.67; H, 5.35. ^{1}H NMR (CD_2Cl_2): δ −14.2 (d of complex m, 1 H, μ-H, $^2J(HP_c)$ = 93 Hz), 0.8 (m, 18 H, $CH_3CH_2P_{d,e}$), 1.2 (m, 12 H, $CH_2P_{d,e}$), 1.9 (m, 9 H, CH_3P_c), 2.2 (m, 6 H, $CH_3CH_2P_c$), 2.5 (complex m, 4 H, diphos), 7.2–7.7 (aromatic H). $^{31}P\{^1H\}$ NMR (CD_2Cl_2): δ −32.0 (d, P_d, $^2J(P_dP_c)$ = 18 Hz), −26.3 (complex m, P_c, $^2J(P_cP_d)$ = 18 Hz, $^2J(P_cP_a)$ = 46 Hz), 68.2 (ddd, P_a, $^1J(P_aRh)$ = 183 Hz, $^2J(P_aP_b)$ = 40 Hz, $^4J(P_aP_c)$ = 46 Hz), 77.8 (ddd, P_b, $^1J(P_bRh)$ = 199 Hz, $^2J(P_bP_a)$ = 40 Hz, $^4J(P_bP_c)$ = 2 Hz).

[(diphos)Rh(μ-H)(μ-Cl)IrH(PEt_3)$_3$]BF_4 (4). To a solution of *mer,cis*-$IrH_2Cl(PEt_3)_3$ (0.210 g, 0.36 mmol) in 20 mL of acetone was added at −20 °C a solution of [(diphos)Rh(acet)$_2$]BF_4 (prepared from 0.240 g (0.36 mmol) of [(diphos)Rh(nbd)]BF_4). The reaction mixture turned red and after 1 h stirring the product was precipitated with pentane and recrystallized from methanol at −20 °C: yield 0.385 g of red crsytals (85%). Anal. Calcd for $C_{44}H_{71}BClF_4IrP_5Rh$: C, 45.07; H, 6.06. Found: C, 45.36; H, 6.00. IR (KBr): ν(Ir–H) 2250 (m) cm^{-1}. ^{1}H NMR (acetone-d_6): δ −21.9 (pseudo q, 1 H, terminal H, $^2J(HP_{d,e})$ = 15.6 Hz), −14.9 (complex m, 1 H, μ-H, $^2J(HP_c)$ = 72.0 Hz, $^2J(HP_a)$ = 31.6 Hz, $^2J(HP_b)$ = 8.9 Hz, $^1J(HRh)$ = 19.7 Hz, $^2J(HP_{d,e})$ = 14.7 Hz), 0.8 (m, 18 H, $CH_3CH_2P_{d,e}$), 1.2 (m, 12 H, $CH_2P_{d,e}$), 1.9 (m, 9 H, CH_3P_c), 2.2 (m, 6 H, $CH_3CH_2P_c$), 2.5 (complex m, 4 H, diphos), 7.4–8.0 (aromatic H). $^{31}P\{^1H\}$ NMR (acetone-d_6): δ −15.0 (d, $P_{d,e}$, $^2J(P_dP_c)$ = 19 Hz), −12.1 (complex m, P_c, $^2J(P_cP_d)$ = 19 Hz), 66.6 (ddd, P_a, $^1J(P_aRh)$ = 184 Hz, $^2J(P_aP_b)$ = 41 Hz, $^4J(P_aP_c)$ = 41 Hz), 74.0 (ddd, P_b, $^2J(P_bRh)$ = 199 Hz, $^2J(P_bP_a)$ = 41 Hz, $^4J(P_bP_c)$ = 3Hz).

[(diphos)Rh(μ-Cl)$_2$IrH($PMePh_2$)$_3$]BF_4 (5). To a solution of *mer,cis*-$IrHCl_2(PMePh_2)_3$ (0.170 g, 0.19 mmol) in THF (10 mL) was added at −78 °C a solution of [(diphos)Rh(acet)$_2$]BF_4 (prepared from 0.134 g of [(diphos)Rh(nbd)]BF_4). After a 2-h stirring at room temperature, concentration of the solution, and addition of pentane, the product precipitated as an orange powder, 0.180 g (67%). The product was only characterized NMR spectroscopically. ^{1}H NMR (CD_2Cl_2): δ −21.8 (pseudo q, 1 H, terminal H, $^2J(HP_{d,e})$ = 14.1 Hz). $^{31}P\{^1H\}$ NMR (CD_2Cl_2): δ −19.7 (br m, P_c), −8.6 (dd, $P_{d,e}$, $^2J(P_dP_c)$ = 9 Hz, $^3J(P_dRh)$ = 16 Hz), 75.8 (dd, P_a, $^2J(P_aRh)$ = 195 Hz, $^2J(P_aP_b)$ = 42 Hz), 78.9 (dd, P_b, $^2J(P_bRh)$ = 187 Hz, $^2J(P_bP_a)$ = 42 Hz).

Reactions of 3 and 4. With CO. Through an acetone-d_6 solution (10 mL) of **3** (0.100 g, 0.083 mmol) was bubbled CO for a few minutes. A $^{31}P\{^1H\}$ NMR measurement showed the presence of the starting $IrHCl_2(PEt_3)_3$ and a "Rh(diphos)" unit. Addition of $NaBPh_4$ (0.028 g, 0.083 mmol) under CO atmosphere afforded a yellow green powder analyzed as [(diphos)Rh(CO)$_3$]BF_4.[12] Anal. Calcd for $C_{53}H_{44}BO_3P_2Rh$: C, 70.37; H, 4.90. Found: C, 70.30; H, 5.11. IR (KBr): 2088 s, 2041 s, 2010 sh m cm^{-1}. $^{31}P\{^1H\}$ NMR (acetone-d_6): δ 60.0 (d, $^2J(PRh)$ = 121 Hz). Compound **4** showed the same reactivity.

With CH_3CN. The addition of an excess of CH_3CN to an acetone-d_6 solution (10 mL) of **3** (0.100 g, 0.083 mmol) was followed by $^{31}P\{^1H\}$ NMR. Formation of the starting $IrHCl_2(PEt_3)_3$ and of a "Rh(diphos)" species was observed. The latter was not isolated, but it is likely to be [(diphos)Rh(CH_3CN)$_2$]BF_4 on the basis of ^{31}P NMR: δ 73.3 (d, $^2J(PRh)$ = 176 Hz).

B. Crystallography. Crystals suitable for X-ray diffraction of both compounds **3** and **4** were obtained as BF_4^- salts by crystallization at −20 °C from methanol. Data were collected on a Nonius CAD4 automatic diffractometer using the parameters listed in Table I with variable scan speed to obtain constant statistical precision on the intensity collected. Data were corrected for Lorentz and polarization factors and absorption with the data reduction programs of the CAD4-SDP package.[13a] Intensities were considered as observed if $I_{net} \geq 3\sigma(I_{tot})$, while an I_{net} = 0.0 was given to those reflections having negative net intensities.

The structures were solved by a combination of Patterson and Fourier methods and refined by block-diagonal least squares as described elsewhere.[13b] No extinction correction was found to be necessary on both sets of data.

Table I. Experimental Data[a] for the X-ray Diffraction Studies

	3	4
formula	$RhIrCl_2P_5C_{44}H_{70}BF_4$	$RhIrClP_5C_{44}H_{71}BF_4$
mol wt	1206.73	1172.28
cryst syst	monoclinic	monoclinic
space group	$P2_1/c$	$P2_1$
a, Å	11.786 (2)	11.102 (2)
b, Å	19.673 (4)	13.582 (3)
c, Å	22.571 (4)	16.694 (4)
β, deg	89.88 (1)	85.06 (2)
Z	4	2
V, Å^3	5233.44	2507.83
ρ(calcd), g cm^{-3}	1.54	1.55
μ, cm^{-1}	31.41	32.06
radiation	Mo K$\bar{\alpha}$ (graphite-monochromated; λ = 0.710 69 Å)	
measd reflcns	$\pm h, +k, +l$	
2θ range, deg	4.5–45.0	5.0–50.0
scan type	$\omega/2\theta$	$\omega/2\theta$
max scan speed, deg min^{-1}	6.7	6.7
scan width, deg	(1.00 + 0.35 tan θ)	(1.10 + 0.35 tan θ)
max counting time, s	35	40
prescan rejectn lim	0.5(2σ)	0.5(2σ)
prescan acceptnce lim	0.03(33σ)	0.02(50σ)
bkgd time	0.5(scan time)	
horiz receiving aperture, mm	2.0 + tan θ	2.0 + tan θ
vert receiving aperture, mm	4.0	4.0
no. of indep data	7844	4880
no. of obsd data [$I \geq 3\sigma(I($]	5750	4553
R^b	0.054	0.062
$R_w{}^c$	0.077	0.089

[a] Collected at room temperature. [b] $R = \Sigma||F_o| - |F_c||/\Sigma|F_o|$. [c] $R_w = [\Sigma w(|F_o| - |F_c|)^2/\Sigma wF_o{}^2]^{1/2}$; $w = 1/(\sigma^2|F_o|)$.

The scattering factors used were from ref 14a, and a correction for the real part of anomalous dispersion was taken into account, using tabulated values.[14a] For compound **4** a correction for the imaginary part was also applied to Ir and Rh atoms.

Structural Studies. [(diphos)Rh(μ-H)(μ-Cl)IrCl(PEt_3)$_3$]BF_4 (3). Crystals of **3** have prismatic habits and are air stable.

A red crystal of approximate dimension 0.3 × 0.2 × 0.4 mm was mounted on a glass fiber for the data collection. From the systematic absences the space group was unambiguously determined as $P2_1/c$.

Cell constants were obtained by least-squares fit of the 2θ values of 25 high-angle reflections ($25.0 \leq 2\theta \leq 36.0$) using the CAD4 centering routines. Crystallographic data and relevant parameters for the data collection are given in Table I.

Three standard reflections ($0\bar{6}8$, $\bar{5}4\bar{1}$, $\bar{2}\bar{8}3$) were used to check the stability of the crystal and the experimental conditions and measured every hour; no significant variation was detected. The orientation of the crystal was checked by measuring two reflections ($\bar{2}8\bar{2}$, $3\bar{7}\bar{4}$) every 250.

An empirical absorption correction was applied by using the azimuthal Ψ scans of reflections $52\bar{1}$, $82\bar{2}$, and $31\bar{1}$. Transmission factors were in the range 0.78–0.97.

The structure was refined by block-diagonal least squares as described above. Upon convergence, the last difference Fourier map showed clearly some of the H atoms bounded to the ligand carbons and a strong peak between the two metal atoms in acceptable position for the μ-H atom.

To check this possibility, a Fourier difference map with a limited data set[15] ((sin θ)/λ cutoff = 0.33 Å^{-1}) was calculated; the presence of a strong peak in the bridging region was confirmed. Therefore, this peak was retained as a μ-H atom and included in the last cycles

---

[12] This product may have been observed by Albano and Aresta by reacting [(diphos)Rh(CO)$_2$]BPh_4 with CO. See: Albano, P.; Aresta, M. *J. Organomet. Chem.* **1980**, *190*, 243.

[13] (a) "Enraf-Nonius Structure Determination Package (SDP)"; Enraf-Nonius: Delft, Holland, 1980. (b) For references to least-squares, Fourier, and structure factor calculation programs, see: Albinati, A.; Brückner, S. *Acta Crystallogr., Sect. B: Struct. Crystallogr. Cryst. Chem.* **1978**, *B34*, 3390.

[14] (a) "International Tables for X-ray Crystallography"; Kynoch Press: Birmingham, England, 1974; Vol. IV. (b) Ibers, J.; Hamilton, W. C. *Acta Crystallogr.* **1964**, *17*, 781.

[15] Teller, R. G.; Bau, R. *Struct. Bonding (Berlin)* **1981**, *44*, 1.

Table II. Positional Parameters for [(diphos)Rh(μ-H)(μ-Cl)IrCl(PEt_3)$_3$]BF_4 (**3**) (Esd's in Parentheses)

	x/*a*	*y*/*b*	*z*/*c*
Ir	0.234 45 (3)	0.114 18 (2)	0.132 15 (2)
Rh	0.188 85 (7)	0.042 59 (4)	0.242 09 (4)
Cl(1B)	0.217 12 (24)	0.161 64 (13)	0.228 76 (12)
Cl(2)	0.248 19 (27)	0.051 75 (16)	0.042 85 (13)
P(1)	0.179 37 (27)	0.036 41 (14)	0.340 02 (14)
P(2)	0.156 48 (24)	−0.067 43 (14)	0.245 03 (13)
P(3)	0.033 30 (27)	0.111 85 (17)	0.118 97 (16)
P(4)	0.427 40 (24)	0.083 61 (16)	0.149 10 (16)
P(5)	0.273 76 (33)	0.220 62 (16)	0.087 75 (16)
C(1B)	0.139 11 (97)	−0.050 84 (62)	0.363 63 (56)
C(2B)	0.187 35 (94)	−0.101 06 (58)	0.319 52 (54)
C(1)Ph(1)	0.077 32 (96)	0.088 69 (61)	0.379 06 (55)
C(2)Ph(1)	0.061 54 (133)	0.080 01 (85)	0.439 96 (76)
C(3)Ph(1)	−0.027 65 (158)	0.119 88 (92)	0.467 89 (88)
C(4)Ph(1)	−0.083 46 (135)	0.166 15 (88)	0.438 46 (77)
C(5)Ph(1)	−0.070 67 (154)	0.176 26 (96)	0.376 31 (87)
C(6)Ph(1)	0.018 78 (137)	0.138 05 (87)	0.352 38 (78)
C(1)Ph(2)	0.310 95 (102)	0.055 78 (65)	0.375 71 (58)
C(2)Ph(2)	0.381 94 (149)	0.006 47 (96)	0.396 96 (84)
C(3)Ph(2)	0.493 31 (169)	0.025 68 (106)	0.419 00 (97)
C(4)Ph(2)	0.521 47 (156)	0.091 06 (98)	0.425 99 (88)
C(5)Ph(2)	0.447 25 (156)	0.137 45 (99)	0.408 16 (88)
C(6)Ph(2)	0.339 47 (132)	0.122 43 (79)	0.383 34 (73)
C(1)Ph(3)	0.229 78 (90)	−0.125 10 (55)	0.195 58 (52)
C(2)Ph(3)	0.216 24 (98)	−0.117 05 (61)	0.135 54 (55)
C(3)Ph(3)	0.270 25 (103)	−0.160 99 (66)	0.093 43 (59)
C(4)Ph(3)	0.338 85 (129)	−0.211 42 (81)	0.116 48 (74)
C(5)Ph(3)	0.355 35 (137)	−0.217 76 (89)	0.174 07 (78)
C(6)Ph(3)	0.299 93 (113)	−0.176 07 (73)	0.215 76 (65)
C(1)Ph(4)	0.005 66 (93)	−0.091 22 (60)	0.234 87 (52)
C(2)Ph(4)	−0.076 98 (111)	−0.047 81 (71)	0.257 82 (64)
C(3)Ph(4)	−0.191 03 (130)	−0.069 15 (85)	0.252 24 (73)
C(4)Ph(4)	−0.221 02 (131)	−0.127 89 (81)	0.226 30 (74)
C(5)Ph(4)	−0.141 70 (124)	−0.167 11 (81)	0.206 77 (72)
C(6)Ph(4)	−0.024 10 (110)	−0.153 90 (70)	0.208 93 (62)
C(1)P(3)	−0.051 98 (136)	0.131 60 (84)	0.186 03 (77)
C(2)P(3)	−0.084 14 (172)	0.195 39 (110)	0.199 48 (99)
C(3)P(3)	−0.040 56 (123)	0.156 38 (80)	0.059 00 (70)
C(4)P(3)	−0.011 29 (148)	0.134 42 (92)	−0.002 45 (86)
C(5)P(3)	−0.008 67 (102)	0.024 62 (65)	0.108 03 (59)
C(6)P(3)	−0.135 78 (134)	0.008 00 (86)	0.094 54 (77)
C(1)P(4)	0.476 86 (161)	0.107 50 (94)	0.223 36 (90)
C(2)P(4)	0.599 69 (205)	0.102 05 (121)	0.244 29 (116)
C(3)P(4)	0.541 96 (130)	0.110 18 (76)	0.100 74 (74)
C(4)P(4)	0.549 20 (154)	0.079 67 (98)	0.040 62 (86)
C(5)P(4)	0.434 68 (111)	−0.008 08 (70)	0.147 38 (63)
C(6)P(4)	0.549 19 (153)	−0.044 84 (99)	0.151 55 (88)
C(1)P(5)	0.386 52 (167)	0.266 62 (109)	0.129 99 (96)
C(2)P(5)	0.392 98 (187)	0.340 46 (123)	0.115 61 (106)
C(3)P(5)	0.165 65 (170)	0.279 13 (109)	0.073 36 (96)
C(4)P(5)	0.111 66 (177)	0.301 68 (112)	0.122 36 (101)
C(5)P(5)	0.347 10 (182)	0.222 87 (118)	0.013 70 (106)
C(6)P(5)	0.293 06 (181)	0.208 39 (115)	−0.039 93 (103)
μ-H	0.199 58 (633)	0.038 64 (403)	0.160 48 (368)
B	0.296 85 (147)	−0.212 47 (88)	0.431 71 (77)
F(1)	0.318 09 (98)	−0.258 50 (66)	0.472 22 (53)
F(2)	0.331 10 (93)	−0.229 10 (57)	0.378 05 (43)
F(3)	0.182 62 (85)	−0.197 63 (55)	0.432 00 (47)
F(4)	0.344 71 (94)	−0.152 97 (57)	0.444 88 (71)

of refinement. The contribution of the remaining hydrogen atoms in their calculated positions (C–H bond lengths = 1.00 Å) was also taken into account but not refined.

Final positional parameters are listed in Table II. Selected bond lengths are given in Table III. Relevant bond angles and internal rotation angles are given in Table IV.

The calculated hydrogen positions (Table A), the thermal factors (Table B), and structure factors (Table C) are given in the supplementary material.

[(diphos)Rh(μ-H)(μ-Cl)IrH(PEt_3)$_3$]BF_4 (4). A deep red crystal of **4** of irregular shape (approximate dimensions 0.3 × 0.4 × 0.4 mm) was mounted on a glass fiber and used for the data collection.

Space group ($P2_1$) and cell constants were obtained as above; relevant informations (crystal and data collection parameters) are given in Table I.

Table III. Bond Lengths (Å) for [(diphos)Rh(μ-H)(μ-Cl)IrCl(PEt_3)$_3$]BF_4 (**3**) and [(diphos)Rh(μ-H)(μ-Cl)IrH(PEt_3)$_3$]BF_4 (**4**)[a] (Esd's in Parentheses)

	3	4
Ir–Rh	2.903 (1)	2.969 (2)
Ir–Cl(1)	2.381 (3)	2.510 (5)
Ir–Cl(2)	2.366 (3)	
Ir–P(3)	2.390 (3)	2.369 (6)
Ir–P(4)	2.384 (3)	2.362 (6)
Ir–P(5)	2.367 (3)	2.245 (7)
Ir–H	1.67 (8)	1.80[b]
Rh–H	1.85 (8)	1.80[b]
Rh–P(1)	2.216 (3)	2.215 (6)
Rh–P(2)	2.199 (3)	2.213 (6)
Rh–Cl(1)	2.386 (3)	2.394 (5)
P(1)–C(1B)	1.86 (1)	1.80 (3)
P(1)–CPh[a]	1.81 (1) ± 0.02	1.85 (2) ± 0.02
P(2)–C(2B)	1.84 (1)	1.87 (3)
P(2)–CPh[a]	1.83 (1) ± 0.02	1.83 (2) ± 0.01
P(3)–C[a]	1.83 (2) ± 0.03	1.78 (3) ± 0.08
P(4)–C[a]	1.82 (1) ± 0.02	1.81 (2) ± 0.03
P(5)–C[a]	1.83 (2) ± 0.07	1.86 (3) ± 0.03
C(1B)–C(2B)	1.51 (2)	1.50 (3)
C–CPh[a]	1.38 (2) ± 0.04	1.37 (4) ± 0.10
C–CEt[a]	1.47 (2) ± 0.08	1.55 (5) ± 0.10
B–F[a]	1.33 (2) ± 0.03	1.36 (4) ± 0.04

[a] Average values. ± refers to the root-mean-square deviation from the mean. A complete list of P–C and B–F bond lengths is given in the supplementary material as Table G. [b] Calculated values. See Experimental Section.

The standard reflections used were $5\bar{2}\bar{2}$, $\bar{1}4\bar{6}$, and 512 to check the crystal decay and the stability and $5\bar{2}3$, $\bar{1}5\bar{6}$, and $5\bar{2}1$ to check the orientation.

Data were corrected for absorption by using the azimuthal Ψ scans of the reflections 4,11,0, 382, and 251; the range of transmission factors was 0.71–0.90.

The structure was refined as above, but no peaks that may be ascribed to the bridging or the terminal hydrogen atoms could be located. The Fourier difference maps with various cutoff limits (down to $(\sin\theta)/\lambda = 0.33$ Å^{-1}) were calculated, but no convincing evidence for them was found.

Therefore, an attempt was made to indirectly locate their positions by minimizing the potential energy[16a,b] of the nonbonded interactions involving the two hydrides with the program HYDEX.[16b] The energy minima found gave reasonable estimates of the positional parameters for the bridging and terminal hydrogen atoms. The Ir–H distances are 1.80 Å for the bridging hydride (constrained by the minimization procedure to be equal to Rh–H) and 1.61 Å for the terminal hydride.

An attempt to include the two hydrides in the least-squares refinement was unsatisfactory and not pursued further.

During the refinement, the contribution of the carbon H atoms in their idealized positions (C–H = 1.08 Å) was taken into account but not refined.

The handedness of the crystal was tested by refining each of the two enantiomorph sets of coordinates. That listed in Table V gave the lower *R* factor and was assumed to represent the correct configuration.[14b]

Final positional parameters are listed in Table V. Selected bond lengths and angles are given in Tables III and IV, respectively. Relevant torsion angles are also in Table IV.

The calculated hydrogen positional parameters (Table D), the thermal factors (Table E), and the structure factors (Table F) are given in the supplementary material.

Results and Discussion

Acetone solutions of [(diphos)Rh(acet)$_2$]BF_4 readily react at −70 °C with *mer,trans*-$IrHCl_2L_3$ to afford, in good yields, the binuclear brick red complexes **1**–**3** as shown in Scheme

---

(16) (a) Ciani, G.; Guisto, D.; Manassero, M.; Albinati, A. *J. Chem. Soc., Dalton Trans.* **1976**, 1943. (b) Orpen, A. G. *J. Chem. Soc., Dalton Trans.* **1980**, 2509.

(17) The relative chemical shift positions of μ-H_{br} and μ-H_{term} are the same as found in other related compounds. See: Boron, P.; Musco, A.; Venanzi, L. M. *Inorg. Chem.* **1982**, *21*, 4192.

Table IV. Selected Bond Angles (deg) and Torsion Angles (deg) for [(diphos)Rh(μ-H)(μ-Cl)IrCl(PEt$_3$)$_3$]BF$_4$ (3) and [(diphos)Rh(μ-H)(μ-Cl)IrH(PEt$_3$)$_3$]BF$_4$ (4) (Esd's in Parentheses)

	3	4
(i) Coordination around Ir		
Ir-H-Rh	111.1 (3.7)	111.0[a]
Ir-Cl(1)-Rh	75.05 (7)	74.5 (1)
Rh-Ir-Cl(1)	52.54 (4)	50.97 (7)
Rh-Ir-Cl(2)	119.26 (6)	
Rh-Ir-H	36.4 (3.2)	34
Rh-Ir-P(3)	85.13 (9)	88.2 (1)
Rh-Ir-P(4)	85.14 (8)	84.3 (2)
Rh-Ir-P(5)	145.79 (3)	152.1 (2)
Cl(1)-Ir-Cl(2)	171.8 (1)	
Cl(1)-Ir-H	88.7 (3.1)	
Cl(2)-Ir-H	89.1 (3.1)	
P(3)-Ir-P(4)	164.1 (1)	159.1 (3)
P(3)-Ir-Cl(1)	92.2 (1)	93.5 (2)
P(3)-Ir-H	77.7 (2.7)	
P(3)-Ir-Cl(2)	87.1 (1)	
P(3)-Ir-P(5)	99.1 (1)	99.0 (2)
P(4)-Ir-Cl(1)	91.8 (1)	96.8 (2)
P(4)-Ir-H	87.0 (2.8)	
P(4)-Ir-P(5)	96.0 (1)	96.8 (2)
P(4)-Ir-Cl(2)	86.7 (1)	
P(5)-Ir-Cl(1)	93.3 (1)	101.5 (2)
P(5)-Ir-Cl(2)	94.9 (1)	
P(5)-Ir-H	176.3 (2.9)	
Ir-P-C[b]	115.6 (5) ± 6.4	118.1 (7) ± 5.6
(ii) Coordination around Rh		
Ir-Rh-Cl(1)	52.41 (4)	54.55 (8)
Ir-Rh-P(1)	152.64 (2)	155.09 (3)
Ir-Rh-P(2)	122.36 (6)	122.04 (9)
Rh-P(1)-C(1B)	110.4 (4)	112.3 (7)
Rh-P(2)-C(2B)	110.2 (3)	110.6 (7)
Cl-Rh-H	85 (3)	
P(1)-Rh-H	174 (3)	
P(1)-Rh-P(2)	84.7 (1)	82.8 (1)
P(1)-Rh-Cl(1)	100.9 (1)	100.6 (2)
P(2)-Rh-H	90 (3)	
P(2)-Rh-Cl(1)	174.0 (1)	176.6 (3)
Rh-P-C(Ph)[b]	116.9 (3) ± 3.7	116.6 (6) ± 2.7
P(1)-C(1B)-C(2B)	108.6 (7)	109.2 (1.4)
P(2)-C(2B)-C(1B)	106.9 (7)	105.2 (1.6)
P-C-CEt[b]	119.1 (6) ± 4.0	115.0 (1.7) ± 4.2
F-B-F[b]	109.4 (1.3) ± 3.9	108.9 (2.0) ± 6.5
(iii) Torsion Angles[c]		
Ir-Rh-P(1)-P(2)	172.3	176.9
Ir-Rh-P(1)-C(1B)	177.1	−176.3
Ir-Rh-P(2)-C(2B)	−157.3	−161.3
Ir-Cl(1)-Rh-P(1)	−174.2	−178.7
Ir-Cl(1)-Rh-P(2)	28.5	−6.8
Rh-Cl(1)-Ir-Cl(2)	2.5	
Rh-Cl(1)-Ir-P(4)	82.4	76.9
Rh-Cl(1)-Ir-P(5)	178.6	175.3

[a] Calculated value. See Experimental Section. [b] Average value. ± refers to the root-mean-square deviation from the mean. A complete list of Rh-P-CPh and F-B-F angles is given in the supplementary material as Table E. [c] Esd's on the internal rotation angles in the range 0.9-1.2° for 3 and 1.9-2.2° for 4.

I. The IR spectra show the typical BF$_4$ bands at ca. 1060 cm^{-1}. No absorption band assignable to a terminal Ir-H vibration could be detected. The ^{1}H NMR spectra of the complexes reveal the presence of a complex multiplet (1 H) centered at ca. −14 ppm (see Table VI), resulting from the coupling between the hydride and P$_a$, P$_b$, and P$_c$ and to Rh. The values of the ^2J(HP$_c$) coupling constants (ca. 90 Hz, see Table VI), obtained in each case by decoupling experiments, are consistent with a *trans*-H-Ir-P$_c$ arrangement. Although the individual ^2J(HP$_a$), ^2J(HP$_b$), and ^1J(HRh) values could not be determined, the complex nature of the hybride multiplet indicates that the hybride ligand is also bonded to rhodium. The occurrence of two doublets for the methyl groups of P$_d$ and P$_e$ in the spectra of complex 1 is due to the diastereotopic nature of the two CH$_3$ groups on P$_d$ and on P$_e$. This is a further indication of bridge formation between the rhodium cation and the iridium moiety in solution.

Scheme I

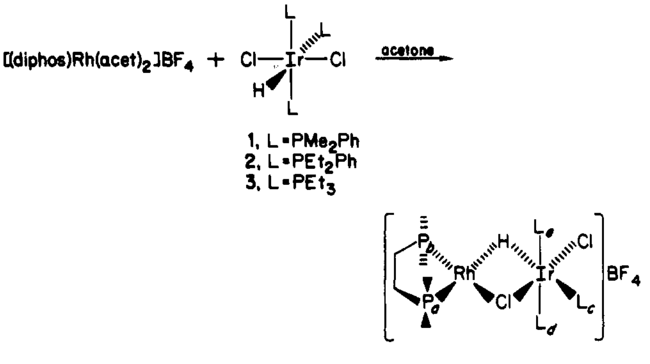

Scheme II

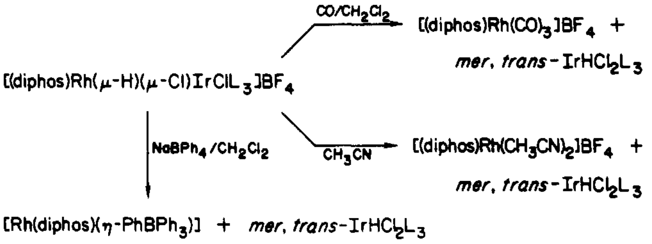

Scheme III

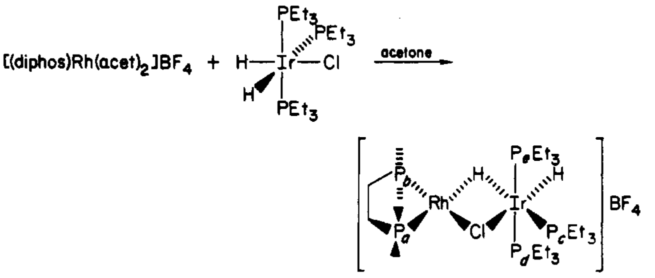

4

The ^{31}P{^{1}H} NMR spectra of complexes 1-3 show four groups of signals (see Table VII). Two of them appear at lower fields and are assignable to P$_a$ and P$_b$. The signal of P$_{d,e}$ is a doublet (^2J(P$_c$P$_{d,e}$) = 15-19 Hz). Those corresponding to P$_a$ and P$_c$ can be assigned unambiguously: thus, by decoupling all protons, except the hydride, only P$_a$ and P$_c$ appear as doublets. It is noteworthy that the trans coupling between the hydride and P$_a$ is 2-3 times smaller than with P$_c$ (see Table VI). This observation could be taken to indicate a better coordination of the bridging hydride toward iridium than rhodium.

Complexes 1-3 readily react with CO, giving mononuclear complexes by displacement of the "IrHCl$_2$L$_3$" moiety (see Scheme II). The poor coordinating power of the bridging atoms toward rhodium prevents the use of solvents with good donor properties, e.g. CH$_3$CN. Cleavage of the "(diphos)Rh" unit is also observed on addition of NaBPh$_4$ to CH$_2$Cl$_2$ solutions of the complexes 1-3. Looking for analogous hydrido-bridged Rh(I)-Ir(III) systems, we have also investigated the reaction of another Ir(III) hydride, namely *mer,trans*-IrH$_2$Cl(PEt$_3$)$_3$ with the "(diphos)Rh" cation. It is interesting to note that, although rhodium shows marked affinity for hydrogen, a (μ-Cl)(μ-H) complex is formed instead for the corresponding (μ-H)$_2$ isomer as shown in Scheme III. This was clearly shown by NMR experiments. Thus, the ^{1}H NMR of 4 reveals the presence of two hydride signals, a complex

Table V. Positional Anisotropic Parameters for $[(\text{diphos})\text{Rh}(\mu\text{-H})(\mu\text{-Cl})\text{IrH}(\text{PEt}_3)_3]\text{BF}_4$ (4) (Esd's in Parentheses)

	x/a	*y/b*	*z/c*
Ir	0.17455 (6)	0.25000 (0)	0.19985 (4)
Rh	0.09222 (15)	0.39709 (14)	0.32426 (10)
Cl	0.08411 (52)	0.22211 (34)	0.34103 (30)
P(1)	0.01831 (57)	0.44594 (46)	0.44525 (34)
P(2)	0.10581 (50)	0.55746 (43)	0.30166 (35)
P(3)	0.37300 (49)	0.26922 (45)	0.23953 (37)
P(4)	−0.00772 (52)	0.28970 (51)	0.14401 (36)
P(5)	0.19000 (54)	0.09522 (50)	0.15293 (38)
C(1B)	−0.00347 (223)	0.57726 (195)	0.45064 (150)
C(2B)	0.09555 (217)	0.62711 (190)	0.39871 (148)
C(1)P(3)	0.40118 (224)	0.39125 (212)	0.28411 (153)
C(2)P(3)	0.51988 (527)	0.41947 (503)	0.30925 (369)
C(3)P(3)	0.48959 (225)	0.26273 (265)	0.15660 (154)
C(4)P(3)	0.48434 (367)	0.36786 (327)	0.09744 (252)
C(5)P(3)	0.44334 (380)	0.21171 (328)	0.31257 (256)
C(6)P(3)	0.38232 (423)	0.21550 (361)	0.40011 (287)
C(1)P(4)	−0.14677 (211)	0.29155 (185)	0.21247 (144)
C(2)P(4)	−0.18876 (242)	0.20191 (214)	0.24932 (164)
C(3)P(4)	−0.00516 (203)	0.41363 (179)	0.10472 (137)
C(4)P(4)	0.09281 (319)	0.43007 (279)	0.02912 (217)
C(5)P(4)	−0.05486 (231)	0.22662 (183)	0.05936 (155)
C(6)P(4)	−0.17053 (284)	0.26860 (296)	0.02391 (194)
C(1)P(5)	0.05640 (266)	0.01306 (228)	0.17609 (183)
C(2)P(5)	0.03808 (313)	−0.02162 (275)	0.26231 (213)
C(3)P(5)	0.20917 (281)	0.07303 (246)	0.04161 (188)
C(4)P(5)	0.33508 (356)	0.12208 (328)	0.00441 (244)
C(5)P(5)	0.31176 (286)	0.01913 (249)	0.18674 (201)
C(6)P(5)	0.31605 (390)	−0.07844 (354)	0.14978 (264)
C(1)Ph(1)	−0.12985 (212)	0.39640 (203)	0.48395 (145)
C(2)Ph(1)	−0.17999 (234)	0.30863 (215)	0.44993 (159)
C(3)Ph(1)	−0.29321 (253)	0.27826 (214)	0.47537 (170)
C(4)Ph(1)	−0.35769 (306)	0.32554 (261)	0.54117 (206)
C(5)Ph(1)	−0.30850 (389)	0.42280 (360)	0.57458 (265)
C(6)Ph(1)	−0.19230 (313)	0.44191 (274)	0.55107 (209)
C(1)Ph(2)	0.11982 (218)	0.41608 (192)	0.52493 (148)
C(2)Ph(2)	0.17212 (328)	0.49326 (297)	0.56483 (227)
C(3)Ph(2)	0.25846 (264)	0.46143 (233)	0.62326 (179)
C(4)Ph(2)	0.28404 (365)	0.36307 (326)	0.63702 (249)
C(5)Ph(2)	0.22626 (276)	0.30711 (254)	0.59685 (187)
C(6)Ph(2)	0.14911 (361)	0.30948 (329)	0.53917 (246)
C(1)Ph(3)	−0.01604 (192)	0.61573 (173)	0.25065 (131)
C(2)Ph(3)	−0.00254 (267)	0.70561 (233)	0.21349 (180)
C(3)Ph(3)	−0.09607 (285)	0.77213 (366)	0.17852 (200)
C(4)Ph(3)	−0.20628 (275)	0.69978 (239)	0.18900 (183)
C(5)Ph(3)	−0.22894 (262)	0.62356 (242)	0.22636 (180)
C(6)Ph(3)	−0.13115 (218)	0.56820 (193)	0.25981 (148)
C(1)Ph(4)	0.23882 (197)	0.60555 (182)	0.24466 (135)
C(2)Ph(4)	0.25757 (251)	0.58770 (219)	0.16330 (168)
C(3)Ph(4)	0.36615 (299)	0.63226 (261)	0.11688 (199)
C(4)Ph(4)	0.44585 (263)	0.68091 (218)	0.15618 (176)
C(5)Ph(4)	0.42580 (322)	0.69628 (284)	0.23694 (216)
C(6)Ph(4)	0.32808 (233)	0.66925 (210)	0.28432 (171)
B	0.65476 (305)	0.97758 (500)	0.13566 (240)
F(1)	0.77642 (204)	0.99853 (250)	0.14360 (194)
F(2)	0.63629 (252)	0.88805 (171)	0.10244 (203)
F(3)	0.59991 (244)	1.00960 (345)	0.20659 (173)
F(4)	0.62595 (329)	1.04896 (182)	0.08806 (197)

multiplet centered at −14.9 ppm, corresponding to the bridging hydride, and a doublet of triplets that is observed as a pseudoquartet (at −21.9 ppm) due to coupling of the terminal hydride with the phosphorus atoms on iridium. Other pertinent NMR data are given in the Experimental Section. It seems to be a general feature of the Rh cation in compounds **1**–**4** to prefer a coordination environment of one chlorine and one hydrogen atom (type A structure) rather than two hydrogen atoms (type B structure).

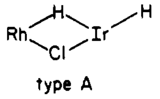

type A

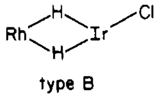

type B

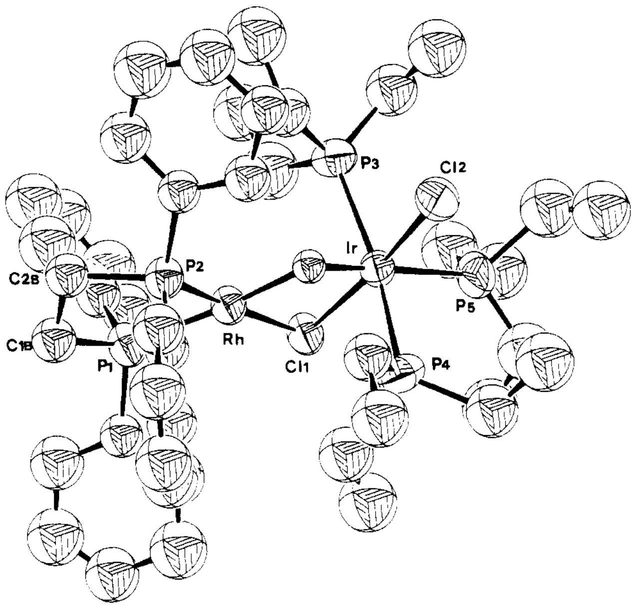

Figure 1. ORTEP view of the cation $[(\text{diphos})\text{Rh}(\mu\text{-H})(\mu\text{-Cl})\text{IrCl}(\text{PEt}_3)_3]^+$ of **3**.

Scheme IV

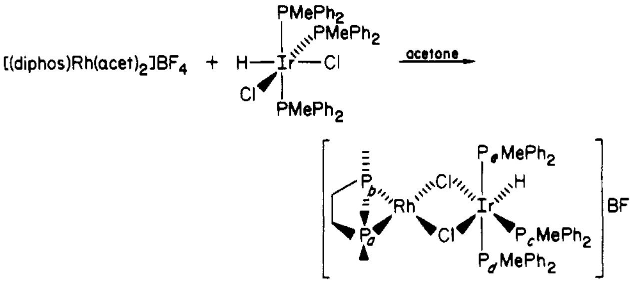

5

The preference for bridging chlorine atoms was also observed in complex **5**, obtained almost quantitatively from *mer,cis*-$\text{IrHCl}_2(\text{PMePh}_2)_3$ and $[(\text{diphos})\text{Rh}(\text{acet})_2]^+$ as shown in Scheme IV. The proposed geometry of **5**, shown in Scheme IV, results from the following:

1. A pseudoquartet (actually an overlapping doublet of triplets) at −21.8 ppm in the ^{1}H NMR spectrum is present, revealing a terminal hydride. It is noteworthy that in all the cationic hydrido-bridged Rh(I)–Ir(III) complexes listed in Table VI bridging hydrides appear at ca. −13 ± 2 ppm. Furthermore, a typical $\nu(\text{IR–H}_{\text{term}})$ band at 2250 cm^{-1} was observed in the IR spectrum.
2. Nonequivalence of the two phosphorus atoms of diphos and the existence of a $^3J(\text{RhP}_{\text{d,e}})$ coupling constant are observed, as shown by the ^{31}P NMR spectrum.

Attempts were made to prepare a complex analogous to **1**–**3** starting from *mer,trans*-$\text{IrHCl}_2(\text{PMePh}_2)_3$. In this case no reaction was observed, as checked by NMR. This should be related to a weaker electron density on the hydride ligand in *mer,trans*-$\text{IrHCl}_2(\text{PMePh}_2)_3$ than in, e.g., *mer,trans*-$\text{IrHCl}_2(\text{PEt}_3)_3$ as the two phosphines have the same cone angle. The difference in electron density is a consequence of the relative donor properties of the two phosphines.[18]

X-ray Structural Studies

(i) Crystal Structures. $[(\text{diphos})\text{Rh}(\mu\text{-H})(\mu\text{-Cl})\text{IrCl}(\text{PEt}_3)_3]\text{BF}_4$ (3). The structure of compound **3** consists of discrete cations and BF_4 anions. An ORTEP[19] view of the cation is given in Figure 1. The relative positions of the metal and

---

[18] Tolman, C. A. *Chem. Rev.* **1977**, *77*, 327.

[19] Johnson, C. K. "ORTEP", Report ORNL-3794; Oak Ridge National Laboratory: Oak Ridge, TN, 1965.

Table VI. Comparison of the Chemical Shifts of Hydrides in Some Cationic Rh(I)-Ir(III) Complexes[17]

	L	solvent	$\delta(H_{br})$	$\delta(H_{term})$	$^2J(\mu\text{-}HP_c)^a$	$^2J(\mu\text{-}HP_c)/{}^2J(\mu\text{-}H_a)^a$
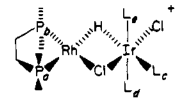	PMe_2Ph (**1**)	CD_2Cl_2	−13.3		93	2.8
	PEt_2Ph (**2**)	CD_2Cl_2	−14.2		90	
	PEt_3 (**3**)	CD_2Cl_2	−14.2		93	2.9
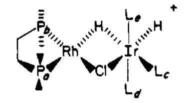	PEt_3 (**4**)	acetone-d_6	−14.9	−21.9	72	2.3
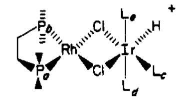	PMe_2Ph (**5**)	CD_2Cl_2		−21.8		
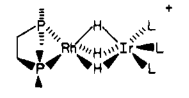	PMe_2Ph (**6**)	acetone-d_6	−10.9			
	$PMePh_2$ (**7**)	acetone-d_6	−10.8			

[a] See text.

Table VII. ^{31}P NMR[a] Data of Complexes **1-5**

		δ (H_3PO_4)				J, Hz							
	L	P_a	P_b	P_c	$P_{d,e}$	P_aRh	P_aP_b	P_aP_c	P_aP_d	P_bRh	P_bP_c	$P_cP_{d,e}$	Δ^b
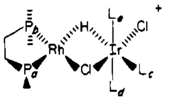	PMe_2Ph (**1**)	68.4	80.5	−38.7	−48.7	182	38	49	3	197	3	19	12
	PEt_2Ph (**2**)	67.0	78.6	−24.8	−31.2	181	42	46	···	198	2	15	10
	PEt_3 (**3**)	68.2	77.8	−26.3	−32.0	183	40	46	···	199	2	18	13
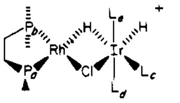	PEt_3 (**4**)	66.6	74.0	−12.1	−15.0	184	41	41	···	199	3	19	
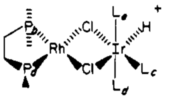	$PMePh_2$ (**5**)	75.8	78.9	−19.7	−8.6	195	42	···	···	187	···	9	

[a] Measured in CD_2Cl_2 for **1-3** and **5** and in acetone-d_6 for **4**. [b] Difference of the $\delta(P_c)$ values of binuclear complexes **1-5** and the corresponding *mer,trans*-$IrHCl_2L_3$.

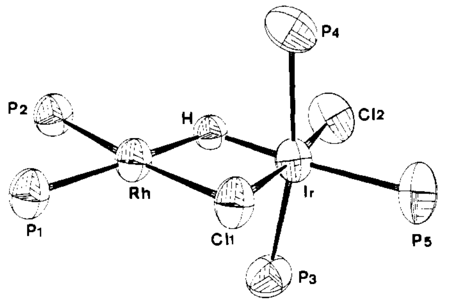

Figure 2. Relative positions of the metal and donor atoms in the cation $[(diphos)Rh(\mu\text{-}H)(\mu\text{-}Cl)IrCl(PEt_3)_3]^+$ of **3**.

donor atoms are shown in Figure 2.

Compound **3** shows a distorted-octahedral coordination around the iridium atom and square-planar geometry around the rhodium atom. The value of the Rh-Ir distance, 2.903 (1) Å, falls in the range found in other bridged bimetallic compounds (2.66-3.01 Å).[15] This distance is comparable with that found in the uncharged complex $[(PEt_3)_2Rh(\mu\text{-}H)(\mu\text{-}Cl)IrH_2(PEt_3)_2]$ (2.899 (1) Å)[4] but longer than that found in $[(diphos)Rh(\mu\text{-}H)_2IrH_2(P\text{-}i\text{-}Pr_3)_2]$ (2.676 (1) Å)[20] and $[(PEt_3)Pt(\mu\text{-}H)_2IrH_2(PEt_3)_2]^+$ (2.680 (1) Å).[21] It is interesting to note that comparable values for the M-M distances are found in the related complexes $[(\eta^5\text{-}C_5Me_5)ClM(\mu\text{-}H)(\mu\text{-}Cl)MCl(\eta^5\text{-}C_5Me_5)]$ (M = Rh, 2.906 (1) Å; M = Ir, 2.903 (1) Å).[22] This is to be contrasted with considerably longer M-M distances observed in the μ-dichloro complexes, which are in the range 3.72-3.77 Å.[22]

The square-planar coordination around the rhodium atom is distorted, the P-Rh-P and P-Rh-Cl(1) angles being 84.7 (1) and 100.9 (1)°, respectively. The Rh-P bonds are different (2.216 (3), 2.199 (3) Å), the longer bond being trans to the bridging hydrogen atom. A similar value (2.197 (2) Å is found in $[(diphos)Rh(\mu\text{-}H)_2IrH_2(P\text{-}i\text{-}Pr_3)_2]$.[20] The geometry of the fragment "Rh(diphos)" is very similar to that reported for $[Rh(diphos)(\eta\text{-}PhBPh_3)]$[23] where a P-Rh-P angle of 84.3 (1)° and Rh-P distances of 2.217 (1) and 2.225 (1) Å have been observed.

The coordination around the iridium atom is that of a distorted octahedron. The pronounced distortion of the P(3)-Ir-P(4) angle (164.1 (1)°) is typical for axial phosphines in related coordination environments; thus, in *mer*-$[IrH_3(PPh_3)_3]$,[24] $[(PPh_3)Au(\mu\text{-}H)IrH_2(PPh_3)_3]^+$,[7] and $[(PEt_3)_2Rh(\mu\text{-}H)(\mu\text{-}Cl)IrH_2(PEt_3)_2]$[4] the *trans*-P-Ir-P angles are 153.0 (3), 149.9 (1), and 166.4 (2)°, respectively. This distortion is likely to arise mainly from the steric repulsions caused by the equatorial ligands. It may be noted that the

---

(20) Musco, A.; Naegeli, R.; Venanzi, L. M.; Albinati, A. *J. Organomet. Chem.* **1982**, *228*, C15.

(21) Emge, T. J.; Koetzle, T. F.; Albinati, A.; Venanzi, L. M. Abstracts, American Crystallography Association Meeting, Columbia, MO, 1983.

(22) Churchill, M. R. *Adv. Chem. Ser.* **1978**, *No. 167*, 36 and references quoted therein.

(23) Albano, P.; Aresta, M.; Manassero, M. *Inorg. Chem.* **1980**, *19*, 1069.

(24) Clark, S. R.; Skelton, B. W.; Waters, T. N. *Inorg. Chim. Acta* **1975**, *12*, 235.

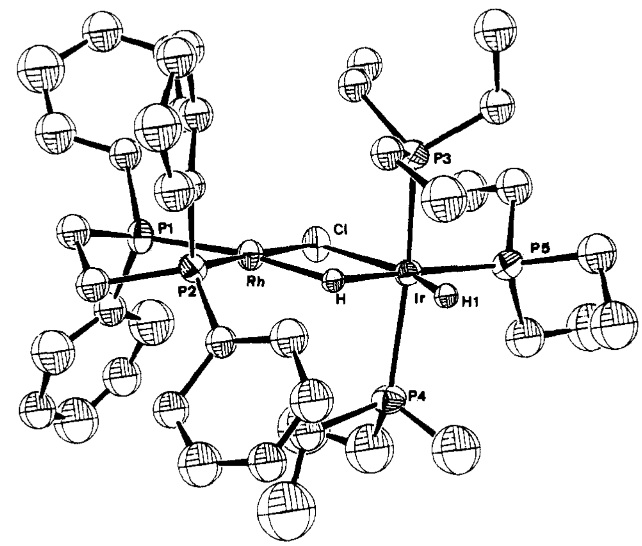

Figure 3. ORTEP view of the cation [(diphos)Rh(μ-H)(μ-Cl)IrH-$(PEt_3)_3]^+$ of **4** (the hydride ligands are shown as spheres of arbitrary size, see text).

axial Ir–P bonds (mean 2.387 (3) Å) are significantly longer than the equatorial Ir–P bond (2.367 (3) Å). A lengthening of the Ir–P bonds, relative to *mer*-$[IrH_3(PPh_3)_3]$, has also been observed upon coordinating the fragment "$Au(PPh_3)$" to an equatorial hydrogen atom of this iridium complex.[7]

The Rh–Cl–Ir bridge is symmetrical (Ir–Cl = 2.381 (3), Rh–Cl = 2.386 (3) Å) and the Rh–Cl–Ir angle, 75.05 (7)°, is in the range expected when an M–M interaction occurs.[22] These values are considerably smaller than those found in the compounds $[(\eta^5\text{-}C_5Me_5)ClM(\mu\text{-}Cl)_2MCl(\eta^5\text{-}C_5Me_5)]$ (M = Rh, Ir), 100.4 (1) and 98.3 (1)°, respectively, where the long M–M distances, 3.719 (1)[25] and 3.769 (1) Å,[26] respectively, practically rule out a direct M–M interaction.

It is noteworthy that the values of the angles Ir–Rh–P(1) and Ir–Rh–P(2) are markedly different (152.64 (2), 122.36 (4)°, respectively). Such differences have been interpreted as indicating an asymmetric bridging situation in related complexes.[6,7] The unambiguous localization and refinement of the bridging hydrogen atom in this compound provides direct support for this assumption. The Rh–H and Ir–H distances (1.85 (8), 1.67 (8) Å) are in the range found in other compounds (1.7–2.1 Å)[19] even though the high esd's associated with the X-ray determination of H positions preclude a detailed discussion of these values. It is to be noted, however, that these distances are consistent with the very different values of ^2J-$(^{31}P,^1H)$, i.e., $^2J(P_cH)/^2J(P_aH)$ = ca. 3, which could also be taken to indicate that the M–H interaction is considerably stronger for iridium than for rhodium.

There are no outstanding features in the geometry of the BF_4 anion. The highly anisotropic thermal motions associated with the fluorine atoms are a common feature for this molecule, which is often disordered in the cell.

(ii) [(diphos)Rh(μ-H)(μ-Cl)IrH$(PEt_3)_3]BF_4$ (4). The structure of compound **4** consists of discrete cationic moieties and BF_4 counterions. An ORTEP[18] view of the cation is given in Figure 3. The relative positions of the metal and donor atoms are shown in Figure 4.

The structure may be described as being built by a distorted-octahedral unit containing iridium(III) and of a square-planar rhodium(I) unit.

The Rh–Ir distance (2.969 (2) Å) is longer than that found in compound **3** (2.903 (1) Å) and falls in the upper range of M–M distances found in binuclear hydrido-bridged complexes.[19]

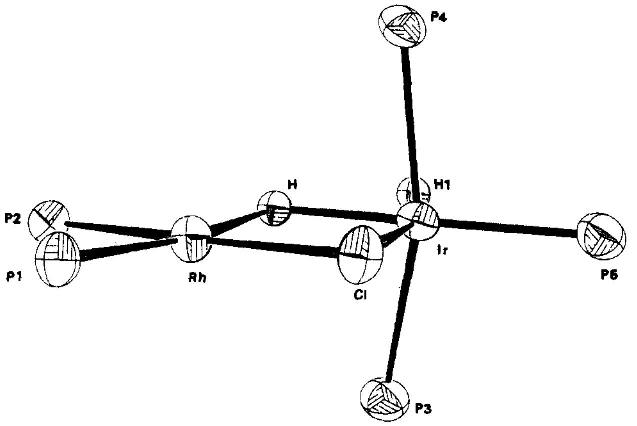

Figure 4. Relative positions of the metal and donor atoms in the cation [(diphos)Rh(μ-H)(μ-Cl)IrH$(PEt_3)_3]^+$ of **4** (the hydride ligands are shown as spheres of arbitrary size, see text).

As expected, the values of the angles P(1)–Rh–P(2), P-(1)–Rh–Cl(1), and P(2)–Rh–Cl(1) (82.8 (1), 100.6 (2), and 176.6 (3)°, respectively) are similar to those found in **3** and show those distortions usually found in square-planar rhodium(I) complexes (see Discussion). However, it should be noted that the two Rh–P distances are equal, with the esd's showing that, in this compound, the bridging H and Cl atoms exert roughly similar trans influences[27] at variance with the results obtained for complex **3**. This difference may be due to differing bonding situations in the two complexes and, particularly, to differences in metal–metal interactions.[28]

The distortions of the octahedron around the iridium atom are of the type usually observed in hydride complexes: Thus, the angles P(5)–Ir–Cl(1) and P(3)–Ir–P(4) have, once again, values (101.5 (2) and 159.1 (2)°, respectively) that are consistent with the idea of repulsions induced by steric interactions caused by the equatorial ligands. It is interesting to note that the Ir–P bond lengths, both axial and equatorial, are shorter than those found in compound **3** (see Table III), possibly indicating a lower electron density at the iridium atom.

The bridging chlorine ligand is in a highly asymmetric environment with a long Ir–Cl bond (2.510 (5) Å) and a shorter Rh–Cl bond (2.394 (5) Å). This is likely to be due to the strong trans influence[27] exerted by the terminal hydride ligand. The Ir–Cl distance may be compared with the value of 2.494 (3) Å found in $[(PEt_3)_2Rh(\mu\text{-}H)(\mu\text{-}Cl)IrH_2(PEt_3)_2]$.[4] However, the Rh–Cl bonds in this compound (2.427 (3) Å is significantly longer than that observed in **3** (see above).

The occurrence of a direct metal–metal interaction in **4** is supported by the value of the Rh–Cl(1)–Ir angle (74.5 (1)°), which is comparable with that found in **3** (75.05 (7) Å).

Although the position of the bridging hydride ligand could not be located, there is an indication for an asymmetric bridging situation from the values of the Ir–Rh–P(1) and Ir–Rh–P(2) angles (155.09 (3) and 122.04 (9)°, respectively), which are very similar to those found in compound **3**.

Also, in this compound, the geometry of the BF_4^- unit is unexceptional and it shows highly anisotropic thermal factors for the fluorine atoms.

Acknowledgment. H.L., D.M., and A.T. received support from the Swiss National Science Foundation and R.T. carried out the work during the tenure of a NATO Fellowship. The authors are greatly indebted to Dr. P. S. Pregosin for valuable

---

[25] Churchill, M. R.; Julis, S. A.; Rotella, F. J. *Inorg. Chem.* **1977**, *16*, 1137.

[26] Churchill, M. R.; Julis, S. A. *Inorg. Chem.* **1977**, *16*, 1488.

[27] Appleton, T. G.; Clark, H. C.; Manzer, L. E. *Coord. Chem. Rev.* **1973**, *10*, 335.

[28] Immirzi, A.; Porzio, W.; Bachechi, F.; Zambonelli, L.; Venanzi, L. M. *Gazz. Chim. Ital.*, in press.

Inorg. Chem. **1984**, *23*, 4261–4265

discussions and thank I. Fecker for some experimental assistance with this work.

Registry No. **1**, 92842-97-2; **2**, 92842-98-3; **3**, 92998-18-0; **4**, 92998-19-1; **5**, 92763-30-9; [(diphos)Rh(acet)$_2$]BF$_4$, 92763-31-0; *mer,trans*-IrHCl$_2$(PMe$_2$Ph)$_3$, 12099-72-8; *mer,trans*-IrHCl$_2$(PEt$_2$Ph)$_3$, 19414-05-2; *mer,trans*-IrHCl$_2$(PEt$_3$)$_3$, 19414-03-0; *mer,cis*-IrH$_2$Cl(PEt$_3$)$_3$, 92842-99-4; *mer,cis*-IrHCl$_2$(PMePh$_2$)$_3$, 22829-32-9; [(diphos)Rh(CO)$_3$]BF$_4$, 92763-33-2; [(diphos)Rh(CH$_3$CN)$_2$]BF$_4$, 92763-35-4.

Supplementary Material Available: Tables containing calculated hydrogen positions for compounds **3** and **4** (Tables A and D), thermal factors (Tables B and E), observed and calculated structure factors (Tables C and F), and bond lengths and angles involving P–C and B–F bonds (Table G) (96 pages). Ordering information is given on any current masthead page.

Contribution from the Department of Chemistry,
University of Odense, DK-5230 Odense M, Denmark

Preparation and Structure of a New Kind of an Extended Partially Oxidized Linear-Chain Compound: *catena*-(μ-Bromo)bis((1*R*,2*R*)-cyclohexanediamine)nickel(2.77) Bromide

HANS TOFTLUND* and OLE SIMONSEN

Received December 20, 1983

The new extended partially oxidized linear-chain nickel compound *catena*-(μ-bromo)bis((1*R*,2*R*)-cyclohexanediamine)nickel(2.77) bromide, [Ni(chxn)$_2$Br]Br$_{1.77}$, has been prepared and characterized by its spectral and magnetic properties. The crystal structure has been determined by single-crystal X-ray analysis using three-dimensional diffractometer data. The compound crystallizes in the orthorhombic space group *I*222 with two formula units in the unit cell. The lattice parameters are $a = 23.544$ (3) Å, $b = 7.095$ (2) Å, and $c = 5.232$ (6) Å. The structure contains chains of Ni(chxn)$_2$ units connected by bromide ions with the Ni–Br distances along the chain = $c/2 = 2.626$ Å. An 11.5% deficiency in the occupation of the bromide counterionic site has been observed, leaving the nickel atoms with an average oxidation state of 2.77. The electronic structure is discussed in the light of the structural, spectral, and magnetic properties.

Introduction

Mixed-valence linear-chain halogenated platinum and palladium amines have received much attention during the last decade, as described in a recent review by Keller.[1]

It has been claimed that nickel forms similar salts; however, there is some confusion about the nature of the halogen-oxidized bis(diamine)nickel complexes. Some have been classified as "tervalent nickel complexes",[2] whereas others have been classified as Ni(II)–Ni(IV) mixed-valence complexes.[3] With some macrocyclic tetraamine ligands, monomeric tervalent nickel complexes are indeed formed.[4]

All reported halogen-oxidized aliphatic nickel complexes have been formulated as stoichiometric compounds, but in the present work we show that at least the bromine-oxidized (1*R*,2*R*)-cyclohexanediamine (chxn) nickel complex is nonstoichiometric and is best described as a partially oxidized nickel(II) system. Although partially oxidized nickel complexes have been reported earlier, all of these are complexes with conjugated π-ligands (e.g. dioximes) oxidized with iodine.[5] The ESR properties of these compounds show that they have not been oxidized at the metal site; rather, they should be classified as Ni(II) complexes with radical ligands. To our knowledge this is the first report on a single-valent nonstoichiometric extended halogen-bridged chain complex.

Experimental Section

Preparation. *catena*-(μ-Bromo)bis((1*R*,2*R*)-cyclohexanediamine)nickel(2.77) Bromide. A solution of [Ni(chxn)$_2$]Br$_2$ in 2-methoxyethanol was prepared by refluxing a mixture of [Ni(chxn)$_3$]Br$_2$[6] (0.64 g, 1 mmol) and anhydrous nickel (II) bromide (0.109 g, 0.5 mmol) for 1 h. The resulting gray solution was placed in a beaker in the diffusion cell. In the bottom of the cell was placed a solution of bromine (0.1 g, 1.25 mmol) in tetrachloromethane (1 mL). Upon this solution was carefully placed a 4-cm layer of dioxane. The cell was closed and kept in the dark for 3 days, during which time dark brown crystals up to 1 mm in size were formed. Anal. Calcd for C$_{12}$H$_{24}$N$_4$Br$_{2.77}$Ni: C, 28.35; H, 5.55; N, 11.02; Br, 43.54; Ni, 11.55. Found: C, 27.90; H, 5.65; N, 10.95; Br, 42.35; Ni, 12.30.

Table I. Crystal Data

orthorhombic *I*222
$a = 23.544$ (3) Å
$b = 7.095$ (2) Å
$c = 5.232$ (6) Å
μ(Mo Kα) = 74.54 cm^{-1}
$V = 874.03$ Å^3

T = room temp
$Z = 2$
mol wt^a = 508.4
ρ(obsd) = 1.95 g cm^{-3}
ρ(calcd) = 1.93 g cm^{-1}

^{a} Molecular weight refers to the asymmetric unit [Ni(C$_6$H$_{12}$N$_2$)$_2$Br]Br$_{1.77}$.

Instrumental Details. The polarized reflectance spectra were recorded on a wide-band reflectometer with a Perkin-Elmer 98 quartz prism monochromator.

Magnetic susceptibility was measured by the Faraday method using Hg[Co(SCN)$_4$] as a standard. The equipment has been described elsewhere.[7]

Raman spectra were obtained from a powder in a pressed KBr plate by using a Jarrell-Ash 25-101 double monochromator. Exciting radiation was provided by a Sp 165-01 krypton laser and a CR argon laser.

The single-crystal X-ray diffraction data were collected from a crystal with the dimensions 0.04 × 0.28 × 0.25 mm by using an Enraf-Nonius CAD4F diffractometer with graphite monochromatized Mo Kα radiation ($\lambda = 0.71073$ Å).

Crystal Data and Intensity Measurements. Unit cell dimensions were obtained from setting angles for 10 reflections.

The results from the least-squares refinement of the cell constants are $a = 23.544$ (3) Å, $b = 7.095$ (2) Å, and $c = 5.232$ (6) Å. The systematic absences indicated four possible space groups: *I*222, *I*2$_1$2$_1$2$_1$, *Imm*2, and *Immm*. The cell dimensions of the related compound [Pt(C$_6$H$_{14}$N$_2$)$_2$Br]Br$_2$ are $a = 23.80$ (2) Å, $b = 7.009$ (6) Å, and c

---

(1) Keller, H. J. In "Extended Linear Chain Compounds"; Miller, J. S., Ed.; Plenum Press: New York, 1982; Vol. I.

(2) Yamashita, M.; Nonaka, Y.; Kida, S.; Hamaue, Y.; Aoiki, R. *Inorg. Chim. Acta* **1981**, *52*, 43.

(3) Papavassiliou, G. C.; Layek, D. *Z. Naturforsch., B: Anorg. Chem., Org. Chem.* **1982**, *37B*, 1406.

(4) Chan, Pui-Ki; Poon, Chung-Kwong. *J. Chem. Soc., Dalton Trans.* **1976**, 858.

(5) Hoffman, B. In: Reference 1, Vol. III.

(6) Laier, T.; Toftlund, H. *Acta Chem. Scand., Ser. A* **1977**, *A31*, 651.

(7) Pedersen, E. *Acta Chem. Scand.* **1972**, *26*, 333.

0020-1669/84/1323-4261$01.50/0